

IRANIAN JOURNAL OF CHEMICAL ENGINEERING

Chairman

Vahid Taghikhani Professor, Sharif University of Technology, Iran

Editor-in-Chief

Seyed Abbas Shojaosadati Professor, Tarbiat Modares University, Iran

Executive Director

Leila Sadafi-Nejad (M. Sc.)

EDITORIAL BOARD

- ❖ Abbasian, J. (Associate Professor, Illinois Institute of Technology, USA)
- ❖ Badakhshan, A. (Emeritus Professor, University of Calgary, Canada)
- ❖ Barikani, M. (Professor, Iran Polymer and Petrochemical Institute, Iran)
- ❖ Jafari Nasr, M. R. (Professor, Research Institute of Petroleum Industry (RIPI), Iran)
- ❖ Karimi, I. A. (Professor, National University of Singapore, Singapore)
- ❖ Madaeni, S. S. (Professor, Razi University, Iran)
- ❖ Mansoori, G. A. (Professor, University of Illinois at Chicago, USA)
- ❖ Moghaddas, J. S. (Professor, Sahand University of Technology, Iran)
- ❖ Moosavian, M. A. (Professor, University of Tehran, Iran)
- ❖ Moshfeghian, M. (Professor, Shiraz University, Iran)
- ❖ Movagharnjad, K. (Associate Professor, Babol University of Technology, Iran)
- ❖ Omidkhah, M. R. (Professor, Tarbiat Modares University, Iran)
- ❖ Pahlavanzadeh, H. (Professor, Tarbiat Modares University, Iran)
- ❖ Panjeshahi, M. H. (Professor, University of Tehran, Iran)
- ❖ Pazouki, M. (Associate Professor, Materials and Energy Research Center (MERC), Iran)
- ❖ Rahimi, R. (Professor, University of Sistan and Baluchestan, Iran)
- ❖ Rashidi, F. (Professor, Amirkabir University of Technology, Iran)
- ❖ Rashtchian, D. (Professor, Sharif University of Technology, Iran)
- ❖ Shariaty-Niassar, M. (Professor, University of Tehran, Iran)
- ❖ Shayegan, J. (Professor, Sharif University of Technology, Iran)
- ❖ Shojaosadati, S. A. (Professor, Tarbiat Modares University, Iran)
- ❖ Soltanmohammadzadeh, J. S. (Associate Professor, University of Saskatchewan, Canada)
- ❖ Towfighi, J. (Professor, Tarbiat Modares University, Iran)
- ❖ Rahimi, M. (Professor, Razi University, Iran)
- ❖ Naseri, S. (Professor, Tehran University of medical Sciences, Iran)

INTERNATIONAL ADVISORY BOARD

- ❖ Arastoopour, H. (Professor, Illinois Institute of Technology, USA)
- ❖ Ataai, M. M. (Professor, University of Pittsburgh, USA)
- ❖ Barghi, Sh. (Assistant Professor, University of Western Ontario, Canada)
- ❖ Chaouki, J. (Professor, University of Polytechnique Montréal, Canada)
- ❖ Ein-Mozaffari, F. (Associate Professor, Ryerson University, Canada)
- ❖ Farnood, R. R. (Professor, University of Toronto, Canada)
- ❖ Jabbari, E. (Associate Professor, University of South Carolina, USA)
- ❖ Jand, N. (Assistant Professor, Università de L'Aquila, Italy)
- ❖ Lohi, A. (Professor, Ryerson University, Canada)
- ❖ Moghtaderi, B. (Professor, University of Newcastle, Australia)
- ❖ Mohseni, M. (Associate Professor, University of British Columbia, Canada)
- ❖ Nassehi, V. (Professor, Loughborough University, UK)
- ❖ Noureddini, H. (Associate Professor, University of Nebraska, USA)
- ❖ Rohani, S. (Professor, University of Western Ontario, Canada)
- ❖ Shahinpoor, M. (Professor, University of Maine, USA)
- ❖ Soroush, M. (Professor, Drexel University, USA)
- ❖ Taghipour, F. (Associate Professor, University of British Columbia, Canada)

* This journal is indexed in the Scientific Information Database (www.SID.ir).

* This journal is indexed in the Iranian Magazines Database (www.magiran.com).

* This journal is indexed in the Islamic World Science Citation Center (www.isc.gov.ir).

Executive Colleague: Fatemeh Hajizadeh & Hamideh Fahimitabar
Editor: Sheryl Nikpoor
Art & Design: Mohsen Alipoor

Iranian Association of Chemical Engineers, Unit 11, No. 13 (Block 3), Maad Building, Shahid Akbari Boulevard, Azadi Ave., Tehran - Iran.

Tel: +98 21 6604 2719 Fax: +98 21 6602 2196

Iranian Journal of Chemical Engineering

Vol. 13, No. 3 (Summer 2016), IACHe

Enhancement of Hydrogen and Methanol Production Using a Double Fluidized-bed Two Membranes Reactor 3-18

M. Bayat, M. R. Rahimpour

Optimization of Candida Rugosa Lipase Immobilization Parameters on Magnetic Silica Aerogel Using Adsorption Method 19-31

L. Amirkhani, J. Moghaddas, H. Jafarizadeh-Malmiri

Mixing of the Immiscible Liquids in the Entrance Region of a T-Type Chamber Using Laser Induced Fluorescence (LIF) Method 32-42

A. A. Sarbanha, F. Sobhanian, S. Movahedirad

Ultrasonic Assisted Synthesis and Characterization of $x\text{CuO}/\text{CeO}_2-\gamma\text{Al}_2\text{O}_3$ Nanocatalysts 43-53

A. Karimi, E. Fatehifar, R. Alizadeh, M. Jamili, A. Jafarizad

Synthesis of 1-(Isopentyloxy)-4-Nitrobenzene Under Ultrasound Assisted Liquid-Liquid Phase-Transfer Catalysis 54-62

P. Abimannan, V. Rajendran

Optimization of Hydrogen Distribution Network by Imperialist Competitive Algorithm 63-77

M. Omidifar, S. Shafiei, H. Soltani

Relationship Between the Microstructure and Gas Transport Properties of Polyurethane/Polycaprolactone Blends 78-88

M. Shahzamani, N. Golshan Ebrahimi, M. Sadeghi, F. Mostafavi

Enhancement of Hydrogen and Methanol Production Using a Double Fluidized-bed Two Membranes Reactor

M. Bayat^{1*}, M. R. Rahimpour²

¹ Department of Chemical Engineering, Faculty of Engineering, University of Bojnord, Bojnord, Iran

² Department of Chemical Engineering, School of Chemical and Petroleum Engineering, Shiraz University, Shiraz 71345, Iran

ARTICLE INFO

Article history:

Received: 2015-12-24

Accepted: 2016-01-30

Keywords:

Ultrapure Hydrogen

Generation

Methanol Enhancement

Fluidized-bed Reactor

Recuperative Coupling

Two-membrane Concept

ABSTRACT

Nowadays, hydrogen and methanol are attractive prospects because of lower emissions compared to the other energy sources and their special application in fuel cell technology, which are now widely regarded as key energy solutions for the 21st century. These two chemicals can also be utilized in transportation, distributed heat and power generation and energy storage systems. In this study, a novel double fluidized-bed two-membrane reactor (DFTMR) is proposed to produce ultrapure hydrogen and enhance methanol synthesis as environmentally friendly fuels, simultaneously. The fluidization concept is used in both sides to overcome drawbacks such as internal mass transfer limitations, pressure drop, radial gradients of concentration and temperature in thermally coupled membrane reactors. The DFTMR system is modeled based on the two-phase theory of fluidization and then its performance is compared with those of thermally coupled membrane reactor (TCMR) and conventional methanol reactor (CR) under the same operating conditions. The simulation results show 24.69% enhancement in hydrogen production in comparison with TCMR. Furthermore, 14.39% and 15.78% improvement in the methanol yield can be achieved compared with TCMR and CR, respectively.

1. Introduction

Most of the energy used today is produced from fossil fuels, which are non-renewable energy sources because they take millions of years to form, and reserves are being depleted much faster than new ones are being made. Nevertheless, the world's dependence on fossil fuels as an energy source leads to serious environmental problems such as the

depletion of natural resources, greenhouse gas emissions and air pollution. Because of these issues, it seems vital to search for alternative methods to produce energy.

1.1. Hydrogen

Hydrogen is a promising, effective and clean energy carrier. It can be prepared in several different ways, such as dehydrogenation,

*Corresponding author: m.bayat@ub.ac.ir

steam-methane reforming, thermo chemical water splitting and high temperature electrolysis [1]. Among these methods, dehydrogenation is an attractive choice for hydrogen production because of its essentially zero carbon dioxide impact, resulting in safe contributions to the environment, and solutions to challenges related to hydrogen storage conditions and medium preparations, such as metal hydrides [2].

Hydrogen fuel cell vehicles can have a lower CO₂ emission and a lower well-to-wheel energy consumption in comparison with advanced diesel/gasoline, or even bio fuel vehicles depending on the hydrogen production pathway. Hydrogen is also considered as a storage medium for surplus electricity generated from fluctuating renewable energies by an electrolyser/storage/fuel cell system.

1.2. Methanol

Methanol is one of the most heavily traded chemical commodities, a material for fuel cell and a kind of transportation fuel. It is one of the cleanest burning fuels and is versatile enough to be used almost anywhere. Moreover, methanol can be used directly by direct methanol fuel cells (DMFCs) [2]. Direct-methanol fuel cells are unique in their atmospheric pressure operation, low temperature, allowing them to be miniaturized to an unprecedented degree. DMFC has several advantages, for instance, very low emissions, high efficiency, potentially renewable fuel source and fast and convenient refueling [3].

1.3. Fluidized-bed membrane reactor

Conventional packed bed reactors are limited because of low catalyst particle effectiveness factors and poor heat transfer as a consequence of catalyst particle size which

leads to severe diffusion limitations [4]. Smaller particle sizes are unfeasible in packed-bed systems because of its unsuitable pressure drop [5]. One of the main advantages of the fluidized-bed reactor is the excellent tube-to-bed heat transfer, which results in efficient and safe operating conditions. In addition, the excellent gas-solid heat transfer characteristics of the fluidized-beds can be effectively used where hot catalysts are circulated between the reactor and the regenerator. By adding membrane in a fluidized-bed, a synergistic effect can be achieved. In this way, the behavior of fluidization can be improved as a result of permeation of gas through the membranes, so significant improvements in conversion and selectivity may be obtained [6].

1.4. Literature review

The importance of methanol has motivated numerous studies with the purpose of improving the efficiency of industrial methanol synthesis reactor. Rahimpour *et al.* [7] studied deactivation of methanol synthesis catalyst and proposed mechanisms for catalyst deactivation. Velardi and Barresi [8] proposed a multi-stage methanol reactor network with auto-thermal behavior to enhance the performance of the reactor. To improve the performance of the methanol reactor, a number of configurations have been suggested including conventional dual-type reactor [9], membrane dual-type reactor [10], fixed bed with hydrogen permselective membrane reactors [11,12], fluidized-bed reactor [13], fluidized-bed membrane dual-type reactors [14] and cascade fluidized-bed membrane reactor [15,16]. In the field of coupling, an adiabatic type of palladium membrane reactor for coupling endothermic and exothermic reactions has been

investigated by Itoh and Wu [17]. A mathematical simulation and numerical method based on a two-dimensional model have been developed by Fukuhara and Igarashi [18] to analyze the operation of the coupling methanol decomposition and methane combustion. In 2009, Khademi *et al.* proposed a membrane thermally coupled reactor (TCMR) that consisted of three sides: methanol synthesis, cyclohexane dehydrogenation and hydrogen production [19]. Methanol synthesis takes place in the exothermic side and provides the required heat for dehydrogenation of cyclohexane, which is an endothermic reaction. Rahimpour and Bayat [20] have investigated a co-current mode for a fluidized-bed thermally coupled membrane reactor to couple methanol synthesis and dehydrogenation of cyclohexane to benzene. Moreover,, they modeled the methanol synthesis and dehydrogenation of cyclohexane to benzene by using a two-membrane thermally coupled membrane reactor [21]. Recently, Bayat *et al.* [22] considered two different configurations of the thermally coupled reactor to enhance methanol production. Their result shows that the exothermic and endothermic reactions should be located in the shell side and tube side, respectively.

1.5. Objectives

The goal of this study is to produce pure hydrogen and enhance methanol yield by employing a double fluidized-bed two-membrane reactor. The catalytic dehydrogenation of cyclohexane to benzene and conversion of synthesis gas to methanol are chosen as the endothermic and exothermic reactions, respectively. The aim is to combine the membrane-assisted selective separation of hydrogen, the coupling of endothermic-

exothermic reactions, in situ water removal and fluidized-bed concept in a single reactor, simultaneously. Moreover, we attempt to demonstrate the advantages of the DFTMR over conventional reactor and thermally coupled membrane reactor (TCMR).

To the best of our knowledge, there is no information available in the literature regarding the use of simultaneous double fluidized-bed thermally coupled reactor and two different membranes (Pd/Ag and H-SOD membrane) for pure hydrogen production and methanol synthesis.

2. Process description

A vertical shell and tube heat exchanger are employed for methanol production, conventionally. The catalysts are packed in vertical tubes and surrounded by the saturated water. The heat, which is generated in exothermic side, is transferred to boiling water and produces steam. The schematic diagram and operating conditions of this reactor have been illustrated in our previous study [21].

The double fluidized-bed two-membrane reactor simulated for simultaneous methanol and hydrogen production is shown in Fig. 1. This novel reactor consists of four concentric tubes. First tube (the inner tube) and fourth tube (the outer tube) are permeation sides while second and third tubes are the exothermic and endothermic sides, respectively. Synthesis gas is fed to the second tube (exothermic side) where methanol synthesis occurs and catalytic dehydrogenation of cyclohexane to benzene is assumed to take place in the third tube (endothermic side), with fluidized beds of different catalysts on both sides. In order to fluidize the catalyst beds, the feed gases are

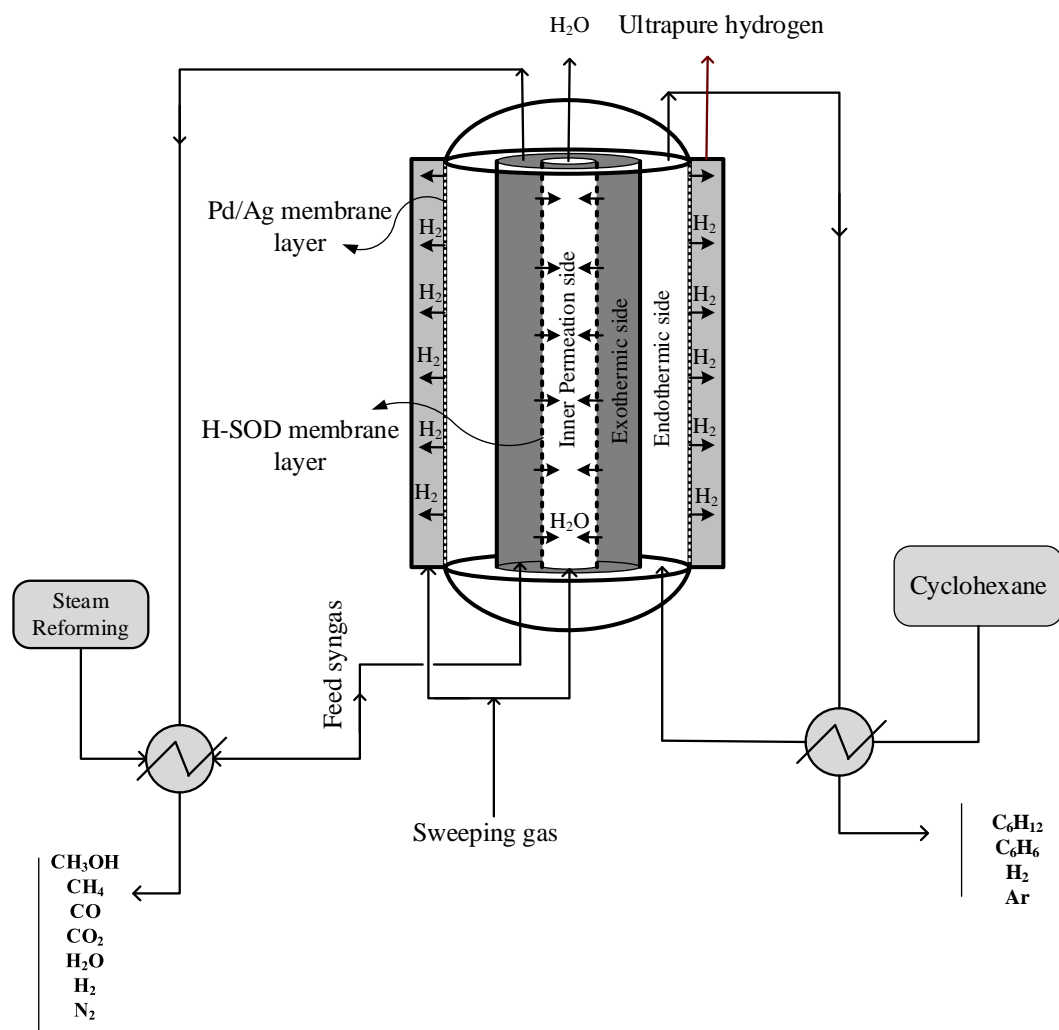


Figure 1. Schematic diagram of the co-current mode for a double fluidized-bed two-membrane reactor (DFTMR).

entered to the bottom of the exothermic and endothermic sides and the catalysts are applied in small sizes. Argon as the sweep gas enters the bottom of permeation sides (first and fourth tubes). The wall between first and second tube is H-SOD membrane and the pressure difference between the two sides of this layer is the driving force for diffusion of water from the exothermic side into the inner permeation side. Therefore, the reacting synthesis gas is cooled simultaneously with the sweep gas in the first tube and the reacting gas in the endothermic side (third tube). Moreover, the wall of the endothermic side is made with a Pd-Ag membrane. Thus, pure hydrogen can penetrate from the endothermic

side into the outer permeation side. The specifications of different sides of DFTMR have been summarized in Table 1. The input data and operating conditions are the same as TCMR [19].

3. Reaction scheme and kinetics

In the conversion of synthesis gas to methanol over commercial $\text{CuO}/\text{ZnO}/\text{Al}_2\text{O}_3$ catalysts, three overall reactions are mainly involved: hydrogenation of carbon monoxide, hydrogenation of carbon dioxide and reverse water-gas shift reaction, which are as follows:

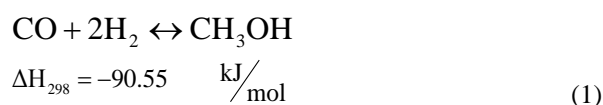
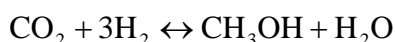


Table 1

The characteristics of DFTMR.

Fluidized bed thermally coupled two-membrane reactor	
Parameter	Value
Inner tube or inner permeation side diameter (m)	0.038
Second tube or exothermic side diameter (m)	0.053
Third tube or endothermic side diameter (m)	0.068
Outer tube or outer permeation side diameter (m)	0.0827
Length of reactor (m)	7.022
Pd/Ag membrane thickness (m)	6×10^{-6}



$$\Delta H_{298} = -49.43 \quad \text{kJ/mol} \quad (2)$$



$$\Delta H_{298} = +41.12 \quad \text{kJ/mol} \quad (3)$$

In the current work, the rate expressions have been selected from Graaf *et al.* [23].

The reaction scheme for the dehydrogenation of cyclohexane to benzene over Pt/Al₂O₃ catalyst is as follows:



$$\Delta H_{298} = +206.2 \quad \text{kJ/mol} \quad (4)$$

The rate expression has been selected from Itoh [24].

4. Mathematical model

4.1. Thermally coupled membrane reactor (TCMR) model

The following assumptions are made during the modeling of a membrane heat exchangers catalytic reactor:

- One-dimensional heterogeneous model is considered (reactions take place in the catalyst particles)
- Steady state condition exists
- Plug flow pattern is assumed in each side
- Axial diffusion of heat and mass are neglected compared with the convection
- There is no radial heat and mass diffusion in catalyst pellet

- Bed porosity in axial and radial directions is constant
- Gas mixtures are assumed to be ideal
- Heat loss is negligible

According to the above assumptions and the differential element along the reactor length, the mole balance equation and the energy balance equations were obtained. The mass balances, energy balances and boundary conditions for solid and gas phases for three sides of reactor are given in Table 2.

4.2. Double fluidized-bed two-membrane reactor (DFTMR) model

Assumptions used for both exothermic and exothermic sides of DFTMR include:

- The dense catalyst bed is considered to be composed of emulsion and bubble phases;
- The bubble and emulsion phases have the same temperature;
- The bubble rise velocity is constant and equal to the average velocity;
- Bubbles are considered to be spherical with constant size;
- The gas in the bubble phase is in plug flow and contains some catalyst particles which take part in reactions, but the extent of reaction in bubble phase is less than emulsion phase.

4.3. Model structure

Fig. 2 depicts a considered length element. On the basis of the above assumptions, the related mass balances, energy balances and boundary conditions for DFTMR are presented in Table 3.

In equations (8) and (14), ζ is equal to 1 for the endothermic side and 0 for the exothermic side. Also, in equation (14), ψ is equal to 0 for the endothermic and 1 for the exothermic side. Moreover, in equations (8) and (14), the positive sign is employed for the

Table 2

Mass and energy balances and boundary conditions for solid and fluid phases in different sides of TCMR.

	Mass and energy balances equation	Number
Solid phase (exothermic and endothermic side)	$a_v c_{ij} k_{gi,j} (y_{i,j}^g - y_{i,j}^s) + \eta r_{i,j} \rho_b = 0$	(5)
	$a_v h_f (T_j^g - T_j^s) + \rho_b \sum_{i=1}^N \eta r_{i,j} (-\Delta H_{f,i}) = 0$	(6)
Fluid phase (exothermic and endothermic side)	$-\frac{F_j}{A_{c,j}} \frac{dy_{i,j}^g}{dz} + a_v c_{ij} k_{gi,j} (y_{i,j}^s - y_{i,j}^g) - \beta \frac{J_{H_2}}{A_{c,j}} = 0$	(7)
	$-\frac{F_j}{A_{c,j}} C_{pj} \frac{dT_j^g}{dz} + a_v h_f (T_j^s - T_j^g) \pm \frac{\pi D_i}{A_{c,j}} U_{1-2} (T_2^g - T_1^g) - \beta \frac{J_{H_2}}{A_{c,j}} \int_{T_2}^{T_3} C_p dT$ $-\zeta \frac{\pi D_i}{A_{c,j}} U_{2-3} (T_2^g - T_3^g) = 0$	(8)
Permeation side	$-F_3 \frac{dy_{i,3}^g}{dz} + \beta J_{H_2} = 0$	(9)
	$-F_3 C_{p3} \frac{dT_3^g}{dz} + \beta J_{H_2} \int_{T_2}^{T_3} C_p dT + \pi D_i U_{2-3} (T_2^g - T_3^g) = 0$	(10)
Boundary conditions	$z = 0 \quad y_{i,j}^g = y_{i0,j}^g, \quad T_j^g = T_{j0}^g, \quad P_j^g = P_{j0}^g \quad j=1,2,3$	(11)

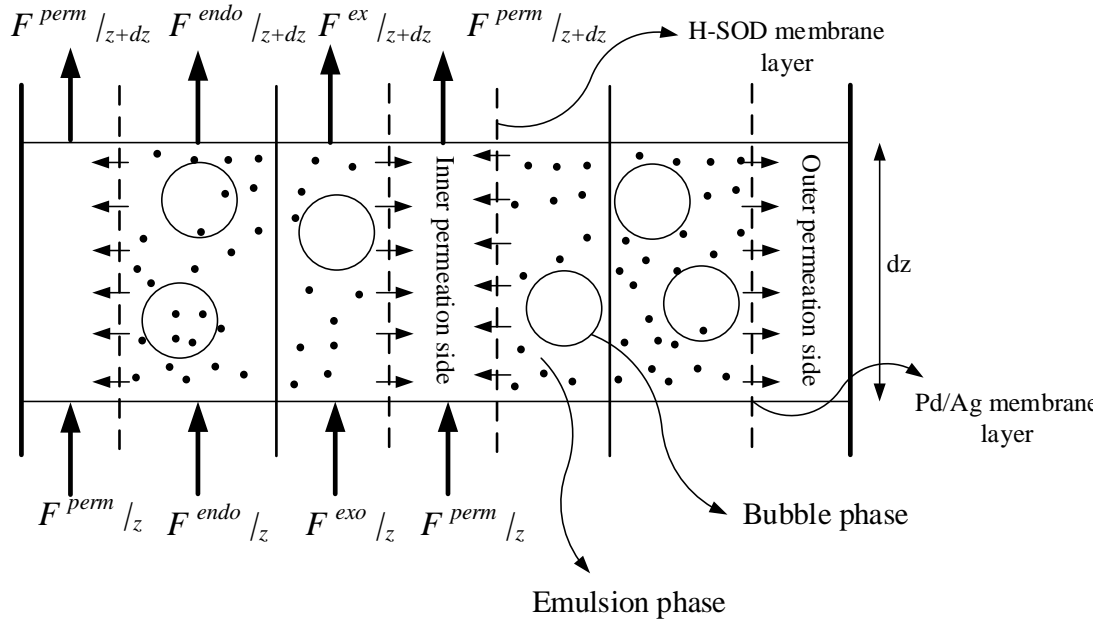


Figure 2. Schematic diagram of an elemental volume of reactor.

exothermic side while the negative sign is used for the endothermic side. β is equal to 1 for hydrogen component and 0 for the other components. In addition, equations (13), (14), (17) and (18) consist of ϕ which is 1 for H₂O

component and 0 for the other components. In the boundary condition equations $y_{i0,j}^g$, T_0^g and P_0^g are the emulsion phase mole fraction of i^{th} component, temperature and pressure at the entrance of j^{th} side of reactor, respectively.

Table 3

Mass and energy balances and boundary conditions for bubble and emulsion phases in different sides of DFTMR.

Mass and energy balances equation	
Bubble phase	$-\frac{\delta}{A_c} \frac{dF_i^b}{dz} + \delta K_{\text{bei}} c_t a_b (y_i^e - y_i^b) + \delta \cdot \gamma \cdot \rho_s \cdot \sum_{j=1}^3 r_{\text{bij}} = 0 \quad F_i^b = y_{ib} F^t \quad (12)$
Emulsion phase	$-\frac{(1-\delta)}{A_c} \frac{dF_i^e}{dz} + \delta K_{\text{bei}} c_t a_b (y_i^e - y_i^b) + (1-\delta) \rho_e \cdot \eta \cdot \sum_{j=1}^3 r_{ij} - \frac{\beta J_{H_2}}{A_{c,j}} - \frac{\phi J_{H_2O}}{A_{c,j}} = 0 \quad F_i^e = y_{ie} F^t \quad (13)$
Energy balance	$-\frac{F_j}{A_{c,j}} C_{pj} \frac{dT}{dz} + (1-\delta) \rho_e \cdot \eta \cdot \sum_{j=1}^3 r_j (-\Delta H_{f,j}) + \delta \cdot \gamma \cdot \rho_b \cdot \eta \cdot \sum_{j=1}^3 r_{bj} (-\Delta H_{f,j}) \pm \frac{\pi D_i}{A_{c,j}} U_{2-3} (T_3^g - T_2^g) - \beta \frac{J_{H_2}}{A_{c,j}} \int_{T_3}^{T_4} C_p dT - \zeta \frac{\pi D_i}{A_{c,j}} U_{3-4} (T_3^g - T_4^g) - \psi \frac{\pi D_i}{A_{c,j}} U_{1-2} (T_1^g - T_2^g) - \phi J_{H_2O} \int_{T_1}^{T_2} C_p dT = 0 \quad (14)$
Outer permeation side	$-F_4 \frac{dy_{i,4}^g}{dz} + \beta J_{H_2} = 0 \quad (15)$
	$-F_4 C_{p4} \frac{dT_4^g}{dz} + \beta J_{H_2} \int_{T_3}^{T_4} C_p dT + \pi D_i U_{3-4} (T_3^g - T_4^g) = 0 \quad (16)$
inner permeation side	$-\frac{F_1}{A_{c,j}} \frac{dy_{i,1}^g}{dz} + \phi J_{H_2O} = 0 \quad (17)$
	$-\frac{F_1 C_{p1}}{A_{c,j}} \frac{dT_1^g}{dz} + \phi J_{H_2O} \int_{T_1}^{T_2} C_p dT + \frac{\pi D_i U_{1-2} (T_2^g - T_1^g)}{A_{c,j}} = 0 \quad (18)$
Boundary conditions	$z = 0 \quad y_{i,j}^g = y_{i0,j}^g, \quad T_j^g = T_0^g, \quad P_j^g = P_0^g \quad j=1,2,3,4 \quad (19)$

The permeation rates of hydrogen and water through the Pd/Ag and H-SOD membranes, respectively, are cited in our previous works [2,21].

Auxiliary equations for the determination of mass transfer coefficients, heat transfer coefficients and hydrodynamic parameters in the proposed model are summarized in Table 4 [25-31].

5. Solution of model

The formulated model consists of ordinary differential equations, the associated boundary conditions and the algebraic equations which are the initial conditions, the

reaction rates, the correlations for the heat and mass transfer coefficients, fluidized-bed hydrodynamic and the physical properties of fluids. In order to solve the aforementioned equations (the set of non-linear differential-algebraic equations) at the steady-state condition, backward finite difference approximation was applied to the system of ordinary differential equations. Then, the reactor length is divided into 100 separate sections and the Gauss-Newton method in MATLAB programming environment is employed to solve the non-linear algebraic equations in each section.

Table 4

Physical properties, mass and heat transfer correlations and the empirical correlations for the hydrodynamic parameters in the proposed model.

Parameter	Equation	Reference
Fixed-bed reactor		
Component heat capacity	$C_p = a + bT + cT^2 + dT^{-2}$	
Mixture heat capacity	$C_{p,m} = \sum_{i=1}^N y_i \times C_{pi}$	
Mass transfer coefficient between gas and solid phases	$k_{gi} = 1.17 \text{Re}^{-0.42} \text{Sc}_i^{-0.67} u_g \times 10^3$ $\text{Re} = \frac{2R_p u_g}{\mu}$ $\text{Sc}_i = \frac{\mu}{\rho D_{im}} \times 10^{-4}$ $D_{im} = \frac{1 - y_i}{\sum_{i=j} y_i D_{ij}}$	Cussler [25]
Overall heat transfer coefficient	$\frac{1}{U} = \frac{1}{h_i} + \frac{A_i \ln(D_o / D_i)}{2\pi L K_w} + \frac{A_i}{A_o} \frac{1}{h_o}$	Wilke [26]
Heat transfer coefficient between gas phase and reactor wall	$\frac{h}{C_p \rho \mu} \left(\frac{C_p \mu}{K} \right)^{2/3} = \frac{0.458}{\varepsilon_B} \left(\frac{\rho u d_p}{\mu} \right)^{-0.407}$	Reid <i>et al.</i> [27] Smith [28]
Fluidized-bed reactor		
Superficial velocity at minimum fluidization	$\frac{1.75}{\varepsilon_{mf}^3 \varphi_s} \left[\frac{d_p \rho_g u_{mf}}{\mu} \right]^2 + \frac{150(1 - \varepsilon_{mf})}{\varepsilon_{mf}^3 \varphi_s} \left[\frac{d_p \rho_g u_{mf}}{\mu} \right] = Ar$	Kunii and Levenspiel [29]
Archimedes number	$Ar = \frac{d_p^3 \rho_g (\rho_p - \rho_g) g}{\mu^2}$ $d_{b,avg} = d_{bm} - (d_{bm} - d_{bo}) \exp(-0.3z / D)$	Kunii and Levenspiel [29]
Bubble diameter	$d_{bm} = 0.65 \left[\frac{\pi}{4} D^2 (u_o - u_{mf}) \right]^{0.4}$ $d_{bo} = 0.376 (u_o - u_{mf})^2$	Mori and Wen [30]
Mass transfer coefficient (bubble-emulsion phase)	$K_{be} = \frac{u_{mf}}{3} + [(4D_{jm} \varepsilon_{mf} u_b / \pi d_b)]^{1/2}$	Sit and Grace [31]
Bubble rising velocity	$u_{b,avg} = u - u_{mf} + 0.711 \sqrt{g d_b}$	Kunii and Levenspiel [29]
Volume fraction of bubble phase to overall bed	$\delta = (u - u_{mf}) / u_b$	Kunii and Levenspiel [29]
Specific surface area for bubble	$a_b = 6\delta / d_b$	
Density for emulsion phase	$\rho_e = \rho_p (1 - \varepsilon_{mf})$	
heat transfer coefficient between bubble and emulsion phase	$h = h_g + h_r + (1 - \delta) \left(\frac{2k_{ew}^0}{d_p} + 0.05 C_{pg} \rho_g u_o \right)$	Kunii and Levenspiel [29]

6. Results and discussions

6.1. Model validation

As stated before, Wagialla and Elshanaie considered a fluidized-bed configuration for methanol synthesis and presented a steady state model based on two-phase theory of fluidization [13]. Table 5 compares the simulated results of our suggested steady state model (FBR) with those from the Wagialla and Elshanaie model. It was observed that, our numerical predictions are in good agreement with the Wagialla and Elshanaie model.

In this section, various steady-state behaviors are analyzed and the predicted components molar flow rate, temperature profiles and methanol yield are presented. The methanol yield and cyclohexane conversion are defined as follows:

$$\text{Methanol yield} = \frac{F_{CH_3OH,out}}{F_{CO,in} + F_{CO_2,in}} \quad (24)$$

$$\text{Cyclohexane conversion} = \frac{F_{C_6H_{12},in} - F_{C_6H_{12},out}}{F_{C_6H_{12},in}} \quad (25)$$

6.2. Temperature trajectory

Fig. 3 shows the temperature profile for conventional methanol reactor (CR), thermally coupled membrane reactor (TCMR) and double fluidized-bed two-membrane reactor (DFTMR) in different sides of the reactor

Table 5

Comparison between simulation and Wagialla and Elshanaie model.

Parameter	Wagialla's model	FBR model	Error (%)
Composition (%)			
CO	1.881	1.79	-4.84
H ₂	73.512	75.38	2.54
CH ₃ OH	4.744	4.92	3.71
CO ₂	2.838	3.12	9.93
H ₂ O	1.809	1.68	-7.131
N ₂	2.356	2.31	-1.95
CH ₄	12.86	11.21	-12.8

configurations. As it can be seen in Fig. 3 (a), controlling the temperature of exothermic side in the DFTMR is easier due to lower hot spot. There is not a sudden increase of temperature for this system at reactor entrance like CR. Furthermore, in the second region, the continually reduced temperature in this bed provides increasing thermodynamic equilibrium potential. Thus, the most favorable exothermic temperature profile seems to belong to DFTMR system owing to simultaneous heat transfer with permeation side in the inner tube and reacting gas in the endothermic side and also using a fluidization concept.

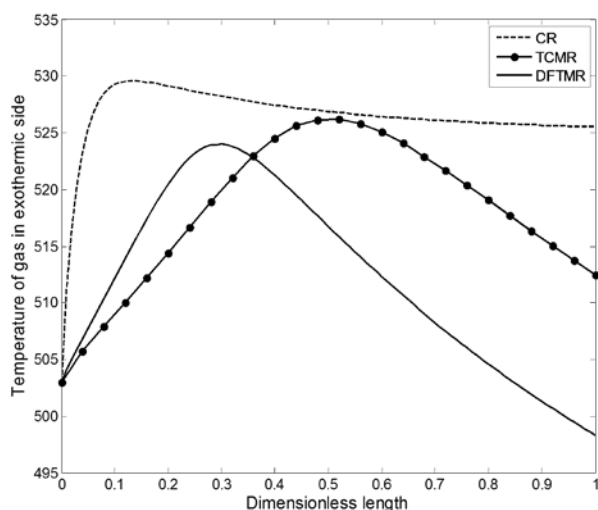
Fig. 3 (b) illustrates the temperature profile for the endothermic sides. As is shown, at the entrance of TCMR, the temperature decreases rapidly and a cold spot forms, then the temperature increases. In situ water removal from the exothermic side to the inner tube in DFTMR shifts the reaction to methanol production, thus more reaction heat is released. Hence, the temperature of DFTMR in the endothermic side is higher than TCMR in reactor entrance region.

The temperature profile of permeation side in DFTMR is higher than that of TCMR. It is due to the excellent heat transfer coefficient because of using fluidized-bed on both sides of the reactor (see Fig. 3 (c)). As this figure shows, the temperature profiles in the outer and inner permeation sides are the same as the temperature profile patterns in reaction sides.

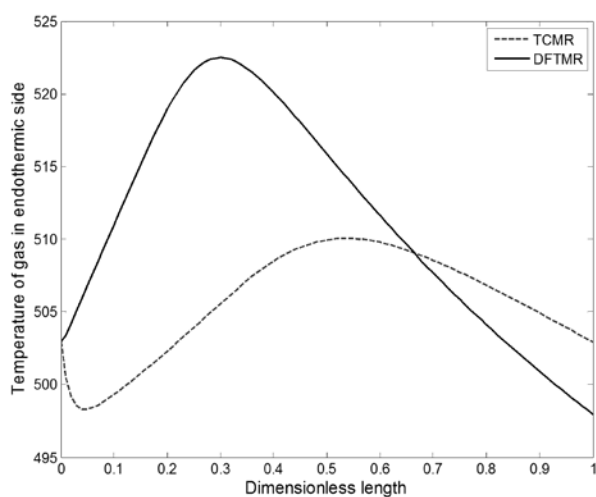
6.3. Molar flow rate behavior

6.3.1. Exothermic side

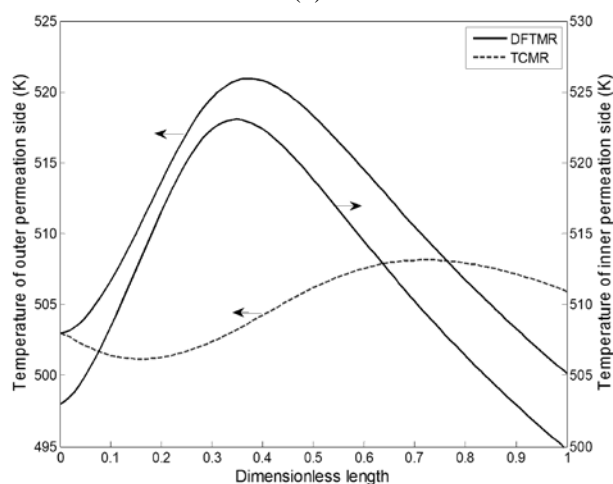
Fig. 4 presents the comparison of methanol molar flow rates in exothermic side of DFTMR with TCMR and CR. These significant differences are due to simultaneous utilization of H-SOD membrane



3(a)



3(b)



3(c)

Figure 3. Variation of temperature for CR and thermally coupled membrane and double fluidized-bed two-membrane reactors in (a) exothermic side, (b) endothermic side, (c) outer and inner permeation sides along the reactor axis.

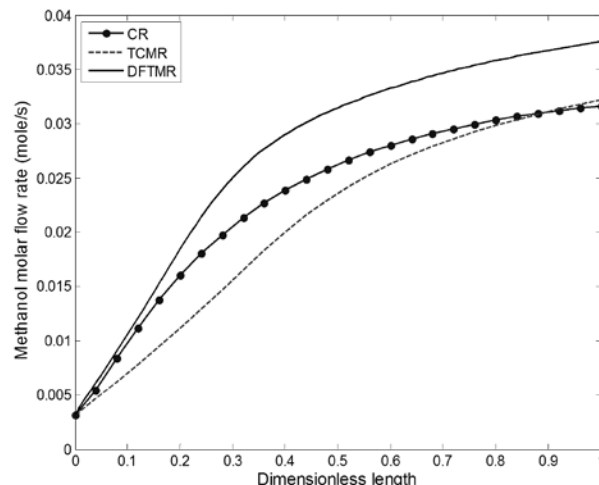


Figure 4. Comparison of methanol molar flow rate along the reactor between exothermic sides of DFTMR, TCMR and CR

and fluidization concept. As it can be seen in this figure, a considerable enhancement of the methanol molar flow rate is achieved by using DFTMR. Using small particles in DFTMR system overcomes mass transfer limitations and leads to a lower pressure drop, therefore, a higher conversion can be attained.

6.3.2. Endothermic side

The molar flow rates of C_6H_6 and H_2 in the endothermic sides of TCMR and DFTMR are illustrated in Figs. 5(a) and (b), respectively. Using the fluidization concept in DFTMR leads to excellent heat transfer, so the endothermic side performs at higher temperature relative to the thermally coupled membrane reactor. Higher molar flow rates of hydrogen and benzene in the endothermic side of DFTMR in comparison with TCMR are achieved as a result of higher temperature profile in this configuration.

6.3.3. Outer permeation side

Hydrogen molar flow rate in outer permeation sides of TCMR and DFTMR is presented in Fig. 6. As seen, there is a considerable enhancement in amounts of hydrogen molar flow rate in DFTMR due to the increase of

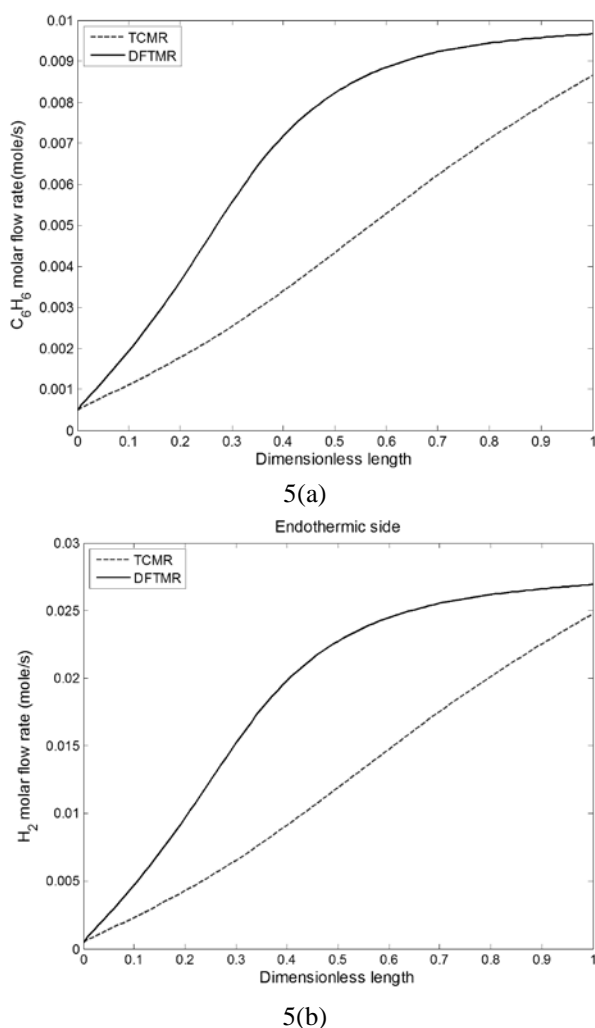


Figure 5. Comparison of (a) C_6H_6 and (b) H_2 molar flow rate along the reactor length between endothermic sides of TCMR and DFTMR.

hydrogen partial pressure in the endothermic side of DFTMR relative to TCMR.

6.4. Comparison of reactors performance

Table 6 compares the performance of the three different reactor types. The effect of utilizing fluidized-bed configuration is obvious in the performance of this novel reactor. The simulated results show 14.39% and 15.78% enhancement in the methanol yield in comparison with TCMR and CR, respectively. Furthermore, the hydrogen recovery yield and cyclohexane conversion (or benzene yield) are improved 24.69% and 11% in the DFTMR compared with the TCMR.

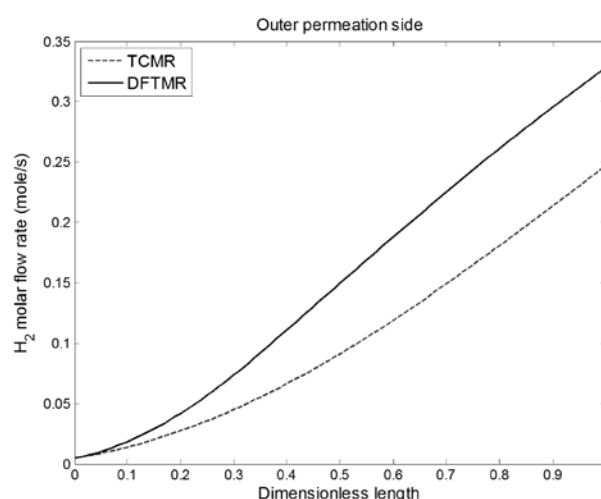


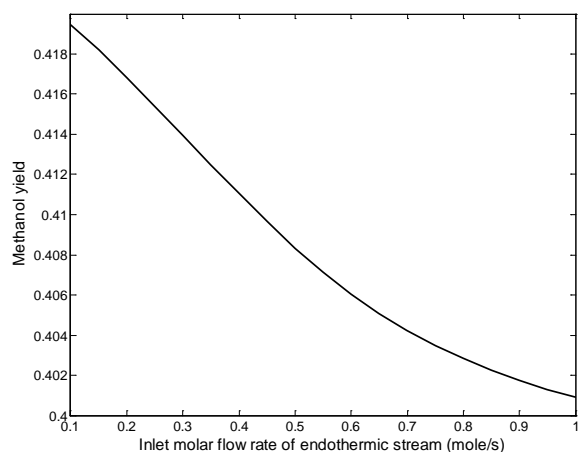
Figure 6. Comparison of hydrogen molar flow rates between outer permeation sides of DFTMR and TCMR.

6.5. Influence of molar flow rate of endothermic stream

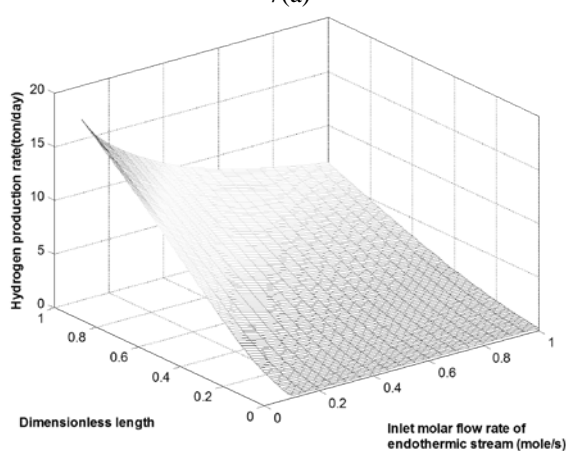
Figs. 7 (a) and (b) demonstrate how the methanol yield and hydrogen production rate behave along the reactor length when the flow rate of endothermic stream increases from 0.1 to 1 mol/s. Fig. 7 (a) shows the reduction of methanol yield with the increasing flow rate of endothermic stream because of lower temperature profile. By increasing the molar flow rate of endothermic stream, the production rate of hydrogen reduces from 16.82 to 6.48, which is due to lower cyclohexane conversion (see Fig. 7 (b)). Decreasing of cyclohexane conversion is an obvious consequence of the fact that the amount of catalyst on endothermic side is not enough for these higher flow rates (see Fig. 7 (c)).

Table 6
Comparison of reactors performance.

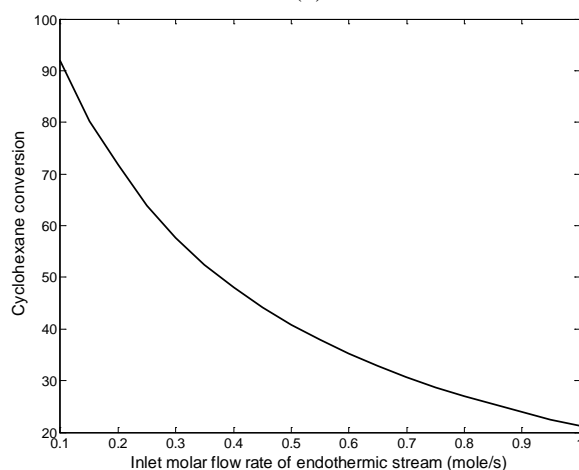
Reactor	Conversion (%)	Yield CH_3OH	Production rate (ton/day)	
	C_6H_{12}		C_6H_6	H_2
CR	-	0.3533	-	-
TCMR	81.59	0.3591	162.85	12.67
DFTMR	91.93	0.4195	182.97	16.82



7(a)



7(b)



7(c)

Figure 7. Influence of molar flow rate of endothermic stream on (a) methanol yield, (b) production of hydrogen and (c) cyclohexane conversion in DFTMR.

6.6. Production rate

Fig. 8 demonstrates the comparison of methanol production in the CR, TCMR and

DFTMR. In order to have a realistic comparison with industrial fixed-bed reactors (CR), the same catalyst loading and operating conditions of an actual industrial reactor are used to simulate the performance of the coupling reactors (TCMR and DFTMR). The methanol production rate in DFTMR is about 65.255 and 59.56 ton/day higher than CR and TCMR, respectively. This considerable development in the methanol production rate is due to utilizing fluidized-bed concept in both reaction sides and two different membranes, simultaneously, which lead to extremely favorable profiles of temperature in both sides of DFTMR.

7. Conclusions

In this work, the performance of a double fluidized-bed two-membrane reactor (DFTMR) was compared with thermally coupled membrane reactor (TCMR) and conventional methanol reactor (CR) under the same operating conditions. One of the main advantages of the fluidized-bed reactor is the excellent tube-to-bed heat transfer, which results in efficient and safe operating conditions even for highly exothermic reactions such as methanol synthesis. The development of a membrane-assisted reactor

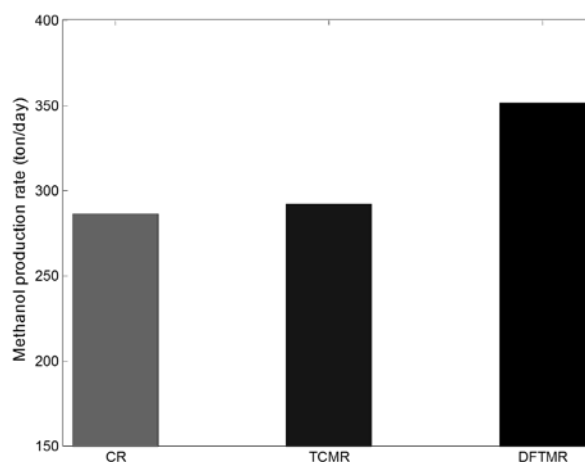


Figure 8. Comparison of methanol production in CR, TCMR and DFTMR.

leads to separation of the hydrogen produced by dehydrogenation reaction. In this way, this recuperative configuration enhances both hydrogen and methanol production, simultaneously. The simulation results show that the temperature profile in exothermic side is favorable for DFTMR and represents a 14.39% and 15.78% enhancement in the methanol yield in comparison with TCMR and CR, respectively. Furthermore, 24.69% and 11 enhancement in the hydrogen and benzene production rate compared to TCMR are achieved, respectively. The simulation results suggest that utilization of double fluidized-bed two-membrane reactor for conversion of synthesis gas to methanol and hydrogen production can be feasible and beneficial. However, the reactor performance needs to be verified experimentally and tested under practical operating conditions.

Nomenclature

A_c	cross section area of each tube (m ²)	F	total molar flow rate (mol/s)
Ar	Archimedes number	h_f	gas-solid heat transfer coefficient (W/m ² .K)
A_i	inside area of inner tube (m ²)	h_i	heat transfer coefficient between fluid phase and reactor wall in exothermic side (W/m ² .K)
A_o	outside area of inner tube (m ²)	h_o	heat transfer coefficient between fluid phase and reactor wall in endothermic side (W/m ² .K)
a_v	specific surface area of catalyst pellet (m ² /m ³)	h_r	radiation heat transfer coefficient (W/m ² .K)
a_b	specific surface area of a bubble (m ² /m ³)	ΔH_{fi}	enthalpy of formation of component i (J/mol)
C_p	specific heat of the gas at constant pressure (J/mol.K)	J_H	permeation rate of hydrogen through the Pd–Ag membrane(mol/m.s)
c_t	total concentration (mol/m ³)	J_{H_2O}	permeation rate of water through the H-SOD membrane(mol/m ³ .s)
D	reactor diameter (m)	K	conductivity of fluid phase (W/m.K)
D_i	tube inside diameter (m)	K_{bei}	mass transfer coefficient for component i in fluidized-bed(m/s)
D_{ij}	binary diffusion coefficient of component i in j (m ² /s)	K_w	thermal conductivity of reactor wall (W/m.K)
D_{im}	diffusion coefficient of component i in the mixture (m ² /s)	k_g	mass transfer coefficient for component i (m/s)
D_o	tube outside diameter (m)	L	reactor length (m)
d_p	particle diameter (m)	M_i	molecular weight of component i (g/mol)
d_b	bubble diameter (m)	N	number of components (N = 6 for methanol synthesis reaction, N = 3 for dehydrogenation reaction)
		P	total pressure (for exothermic side: bar; for endothermic side: Pa)
		P_i	partial pressure of component i (Pa)
		Re	Reynolds number
		R_p	particle radius (m)
		r_i	reaction rate of component i (for exothermic reaction: mol/kg.s; for endothermic reaction: mol/m ³ .s)
		Sc_i	Schmidt number of component i
		T	temperature (K)
		U	overall heat transfer coefficient between exothermic and endothermic sides (W/m ² .K)
		u	superficial velocity of fluid phase (m/s)
		u_b	velocity of rising bubbles (m/s)
		u_g	linear velocity of fluid phase (m/s)
		v_{ci}	critical volume of component i (cm ³ /mol)

y_i mole fraction of component i (mol/mol)

z axial reactor coordinate (m)

Greek letters

γ volume fraction of catalyst occupied by solid particle in bubble

δ bubble phase volume as a fraction of total bed volume

ε_B void fraction of catalytic bed

ε_{mf} void fraction of catalytic bed at minimum fluidization

η catalyst effectiveness factor

μ viscosity of fluid phase (kg/m·s)

ρ density of fluid phase (kg/m³)

Superscripts and Subscripts

0 inlet conditions

1 inner tube

2 exothermic side

3 endothermic side

4 outer tube

B catalytic bed

b bubble phase

e emulsion phase

g in bulk gas phase

i chemical species

j reactor side

k reaction number index

s at surface catalyst

Abbreviations

CR conventional reactor

TCMR thermally coupled membrane reactor

DFTMR double fluidized-bed two-membrane reactor

References

- [1] Demir, N., "Hydrogen production via steam-methane reforming in a SOMBRERO fusion breeder with ceramic fuel particles", *Int. J. Hydrogen Energy*, **38**, 853 (2012).
- [2] Bayat, M. and Rahimpour, M. R., "Production of hydrogen and methanol enhancement via a novel optimized thermally coupled two-membrane reactor", *Int. J. Energy Res.*, **37**, 35 (2013).
- [3] Oliveira, V. B. Falcao, D. S. Rangel, C. M. and Pinto, A. M. F. R., "A comparative study of approaches to direct methanol fuel cells modeling", *Int. J. Hydrogen Energy*, **32**, 415 (2007).
- [4] Adris, A. M. Elnashaie, S. S. E. H. and Hughes, R., "A Fluidized Bed Membrane Reactor for the Steam Reforming of Methane", *Can. J. Chem. Eng.*, **69**, 1061 (1991).
- [5] Santos, A. Mene'ndez, M. and Santamaria, J., "Partial oxidation of methane to carbon monoxide and hydrogen in a fluidized bed reactor", *Catal. Today*, **21**, 481 (1994).
- [6] Deshmukh, S. A. R. K. Heinrich, S. Mörl, L. van Sint Annaland, M. and Kuipers, J. A. M., "Membrane Assisted Fluidized-bed Reactors: Potentials and Hurdles", *Chem. Eng. Sci.*, **62**, 416 (2007).
- [7] Rahimpour, M. R. Fathikalajahi, J. and Jahanmiri, A., "Selective kinetic deactivation model for methanol synthesis from simultaneous reaction of CO₂ and CO with H₂ on a commercial Copper/zinc oxide catalyst", *Can. J. Chem. Eng.*, **76**, 753 (1988).
- [8] Velardi, S. A. and Barresi, A. A., "Methanol synthesis in a forced unsteady-state reactor network", *Chem. Eng. Sci.*, **57**, 2995 (2002).
- [9] Rahimpour, M. R. and Lotfinejad, M., "A comparison of co-current and counter-current modes of operation for a dual type industrial methanol reactor", *Chem. Eng. Process*, **47**, 1819 (2008).
- [10] Rahimpour, M. R. and Alizadehhesari, K., "Enhancement of carbon dioxide removal in a hydrogen-permselective methanol synthesis reactor". *Int. J. Hydrogen Energy*, **34**, 1349 (2009).
- [11] Rahimpour, M. R. Khosravanipour Mostafazadeh, A. and Barmaki, M. M.,

- "Application of hydrogen-permselective Pd-based membrane in an industrial single-type methanol reactor in the presence of catalyst deactivation", *Fuel Process. Technol.*, **89**, 1396 (2008).
- [12] Rahimpour, M. R. and Ghader, S., "Enhancement of CO conversion in a novel Pd-Ag membrane reactor for methanol synthesis", *Chem. Eng. Process*, **43**, 1181 (2004).
- [13] Wagialla, K. M. and Elnashaie, S. S. E. H., "A fluidized-bed reactor for methanol synthesis .a theoretical investigation", *Ind. Eng. Chem. Res.*, **30**, 2298 (1991).
- [14] Rahimpour , M. R. and Bayat, M., "Comparative study of two different hydrogen redistribution strategies along a fluidized-bed hydrogen permselective membrane reactor for methanol synthesis", *Ind. Eng. Chem. Res.* **49**, 472 (2010).
- [15] Rahimpour, M. R. Bayat, M. and Rahmani, F., "Enhancement of methanol production in a novel cascading fluidized-bed hydrogen permselective membrane methanol reactor", *Chem. Eng. J.*, **157**, 520 (2010).
- [16] Rahimpour, M. R. Bayat, M. and Rahmani, F., "Dynamic simulation of a cascade fluidized-bed membrane reactor in the presence of long-term catalyst deactivation for methanol synthesis", *Chem. Eng. Sci.* **65**, 4239 (2010).
- [17] Itoh, N. and Wu, T. H., "An adiabatic type of palladium membrane reactor for coupling endothermic and exothermic reactions", *J. Membr. Sci.* **124**, 213 (1997).
- [18] Fukuhara, C. and Igarashi, A., "Performance simulation of a wall type reactor in which exothermic and endothermic reactions proceed simultaneously, comparing with that of a fixed bed reactor", *Chem. Eng. Sci.*, **60**, 6824 (2005).
- [19] Khademi, M. H. Jahanmiri, A. and Rahimpour, M. R., "A novel configuration for Hydrogen production from coupling of methanol and benzene synthesis in a hydrogen perm selective membrane reactor", *Int. J. Hydrogen Energy*, **34**, 5091 (2009).
- [20] Rahimpour, M. R. and Bayat, M., "Production of ultrapure hydrogen via utilizing fluidization concept from coupling of methanol and benzene synthesis in a hydrogen permselective membrane reactor", *Int. J. Hydrogen Energy*, **36**, 6616 (2011).
- [21] Bayat, M. and Rahimpour, M. R., "Simultaneous utilization of two different membranes for intensification of ultrapure hydrogen production from recuperative coupling autothermal multitubular reactor", *Int. J. Hydrogen Energy*, **36**, 7310 (2011).
- [22] Bayat, M. Rahimpour, M. R. Taheri, M. Pashaei, M. and Sharifzadeh, S., "A comparative study of two different configurations for exothermic-endothermic heat exchanger reactor", *Chem. Eng. Process*, **52**, 63 (2012).
- [23] Graaf, G. H. Scholtens, H. Stamhuis, E. J. and Beenackers, A. A. C. M., "Intra-particle diffusion limitations in low-pressure methanol synthesis", *Chem. Eng. Sci.*, **45**, 773 (1990).
- [24] Itoh, N., "A membrane reactor using palladium", *AIChE J.*, **33**, 1576 (1987).
- [25] Cussler, E. L., Diffusion, mass transfer in fluid systems, Cambridge University Press, (1984).
- [26] Wilke, C. R., "Estimation of liquid diffusion coefficients", *Chem. Eng. Progress*. **45**, 218 (1949).
- [27] Reid, R. C., Sherwood, T. K. and Prausnitz, J., The properties of gases and

- liquids, 3rd ed. New York: McGraw-Hill, (1977).
- [28] Smith, J. M., Chemical engineering kinetics, New York, McGraw-Hill, (1980).
- [29] Kunii, D. and Levenspiel, O., Fluidization engineering, New York, Wiley, (1991).
- [30] Mori, S. and Wen, C. Y., "Estimation of bubble diameter in gaseous fluidized beds", *AIChE J.*, **21**, 109 (1975).
- [31] Sit, S. P. and Grace, J. R., "Effect of bubble interaction on interphase mass transfer in gas-fluidized beds", *Chem. Eng. Sci.*, **36**, 327 (1981).